Possible evidence for stochastic acceleration of electrons in solar hard X-ray bursts observed by *SMM*

John C. Brown and Jon M. Loran *Department of Astronomy, The University, Glasgow G12 8QQ*

Summary. It is shown that the dynamic, hard X-ray spectra of the events of 1980 March 29 and June 7 observed by the *Solar Maximum Mission* (HXRBS) exhibit an anticorrelation of photon flux and spectral steepness. This is exhibited in terms of systematic loci followed by the event in the plane (flux I, spectral index γ). These observations are compared with a theoretical model, developed from Benz, involving injection of electrons into a thick target region from a fluctuating slab in which they are stochastically accelerated. The data are found to be in reasonable accord with the model predictions and are used to obtain constraints on plasma conditions in the acceleration site. Theoretical implications of this result are discussed, as are possible sources of deviation between the data and the theory.

1 Introduction

Observations of dynamic spectra of solar hard X-ray bursts can be used to infer the properties of energetic electron production in the source (e.g. Brown 1971; Kane 1974; Melrose & Brown 1976; Brown & Hoyng 1975; Hudson, Canfield & Kane 1978). In particular correlations between variations in burst flux and spectral hardness place constraints on permissible source models. Such correlations were first reported by Kane & Anderson (1970) — and subsequently by Hoyng, Brown & van Beek (1976), Crannell *et al.* (1978) and others — and most commonly take the form of a positive correlation of flux with spectral hardness (i.e. with temperature T for thermal spectral models and inversely with spectral index γ for power-law spectral models). They are best displayed in terms of the locus traced through the event in the plane of flux versus spectral index (or temperature).

Most recently, Kiplinger *et al.* (1983) have reported such a correlation between flux and spectral hardness in the hard X-ray flare of 1980 June 7 observed by the *SMM* Hard X-ray Burst Spectrometer (HXRBS). Of particular interest is the fact that the same general form of the correlation is repeatedly traced out during each of the seven intense spikes which characterize the main part of the event. (For full details of this interesting event, the reader is referred to Kiplinger *et al.* 1983, and also to the report by Kane *et al.* 1983, of independent observations.) In a study of somewhat similar repeated correlation structure in the event of

246   *J. C. Brown and J. M. Loran*

1972 August 4, Benz (1977) proposed that the behaviour could be explained in terms of a thick target model in which the electrons are stochastically accelerated in a fluctuating region filled with Langmuir waves. In this paper we examine a small sample of HXRBS events for evidence of this dynamic spectral behaviour and in particular compare results for the events of 1980 March 29 and June 7 with the predictions of the Benz-type model.

2 The data

We have available to us a small sample of the HXRBS data set kindly supplied by the HXRBS team and have examined our events for evidence of the type of anticorrelation between flux (I) and spectral index γ discussed above. To do so we have used a simple 2-channel power-law spectral fitting procedure, incorporating detector efficiency curves, which we find gives ample agreement near the peak of intense events ($\Delta\gamma \simeq \pm 0.3$) with published power-law fits incorporating the full detector response. We recognize that a single power-law is not always the best fit to the data (*cf.* Kiplinger *et al.* 1983) but are concerned here only with a first-order measure of the spectral hardness and its variations, for comparison with a theory which itself only gives first-order estimates.

In all the events we examined (1980 March 29; April 10; May 9; May 21; June 7; November 5) we found an overall tendency for I and γ to anticorrelate but also that the instant by instant changes in $I(t)$, $\gamma(t)$ often followed a rather complex path in the (γ, I) plane. [Kiplinger (personal communication) advises us that this trend holds for the majority of HXRBS events, though with a few notable counter examples.) However the events of March 29 and June 7 not only showed an anticorrelation between I and γ but through much of their duration followed a well-defined path in the γ, I plane. We have selected these for comparison here with the Benz model and we defer consideration of the more complicated (γ, I) events for future study but presume that they represent either a different mechanism of electron production or the superposition of a number of electron production sites.

In Fig. 1 we show the time profile of the March 29 event in the energy band 32–54 keV. This consisted chiefly of a single very intense impulsive spike (*cf.* Dennis, Frost & Orwig 1981) with comparatively little structure preceded by a minor peak of about 10 per cent of the flux. In Fig. 2 we show the computed dynamic spectral locus in the plane of I_* (total power-law flux above 32 keV) versus γ computed from the ratio $I(32–54\,\text{keV})/$
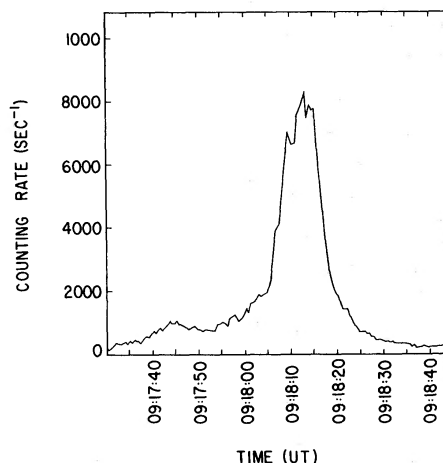

Figure 1. Time profile of the intense spike hard X-ray burst of 1980 March 29 in the HXRBS energy channel 32–54 keV plotted with 512 ms integration interval.
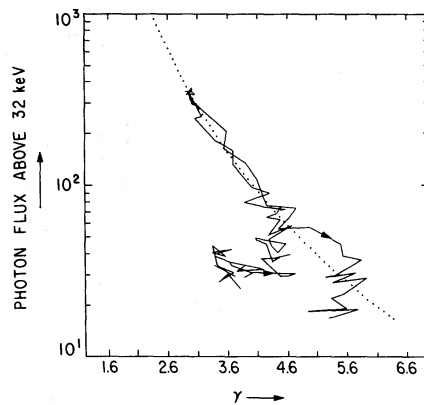
Figure 2. Locus of I_* (cm^{-2}s^{-1}) (with $\epsilon = E_* = 32$ keV) versus γ for the event of 1980 March 29 between UT 09:17;40 and 09:18:30. Superposed (dashed line) is the best fit theoretical curve predicted by the stochastic acceleration model.

I(77–101 keV). The closeness of the data locus to a single path is very striking, particularly in relation to the superposed (dashed) theoretical curve (*cf.* Section 3), aside from the very beginning and end portions.

In Fig. 3 we show the whole time profile of the June 7 event, in the 32–54 keV energy channels while in Fig. 4 we show the expanded time profiles in this channel, and in the 77–101 keV channel for the section containing the seven spikes which dominate the initial part of the event impulsive phase (Kiplinger *et al.* impulsive phase 1). Fig. 4 also shows the fitted $\gamma(t)$ for this section and indicates the anticorrelation with $I(t)$. To show this anticorrelation explicitly, and its degree of consistency from spike to spike, we have divided the time interval of Fig. 4 into nine portions shown by the dot-dashed lines and labelled (a)–(i) where (a) comprises the initial rise, (b)–(h) the seven main spikes, and (i) the rest of the event including the second and third sets of weaker impulsive spikes reported by Kiplinger *et al.* (*cf.* fig. 3). For each of these nine portions, we have constructed the locus of $I_*(t)$ (again above 32 keV) versus $\gamma(t)$ with the results shown in Fig. 5(a)–(i). Here we will be chiefly concerned with the systematic trend of the (γ, I) locus for the seven main spikes, labelled (b)–(h) in Fig. 5. We note also, however, that during the second and third sets of spikes, anticorrelation loci are performed of generally similar form, but on a reduced I scale, as
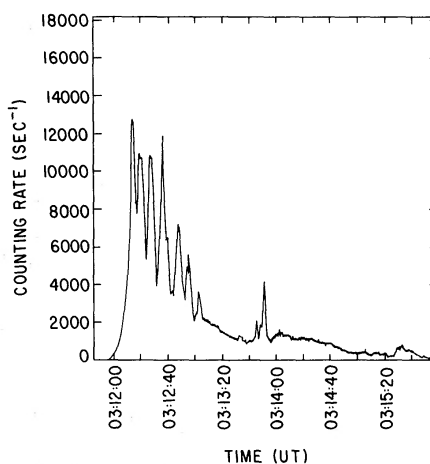

Figure 3. Time profile of the entire multiple spike hard X-ray burst of 1980 June 7 in the HXRBS energy channel 32–54 keV plotted with 512 ms integration interval.
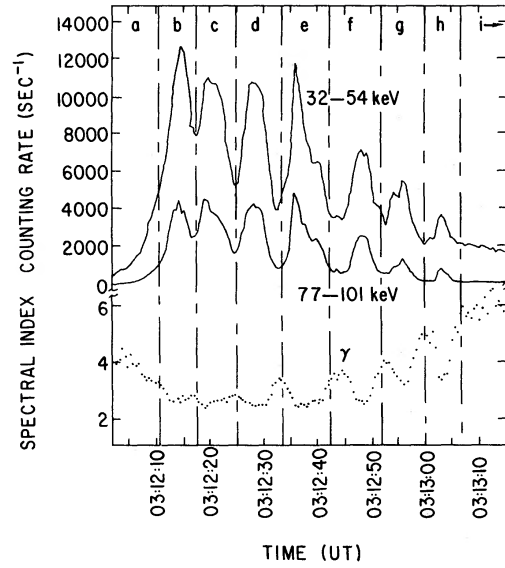
248   *J. C. Brown and J. M. Loran*

Figure 4. Expanded time profile of the seven main spikes of the June 7 event in energy channels 32–54 keV and 77–101 keV together with the evolution of the power-law spectral index γ obtained from the ratio of these channels. Note the anticorrelation of γ and count rate. The subdivision of the time interval corresponds to that used in Fig. 5, subdivision (i) extending to UT 03:16:00.

distinct from the much more chaotic behaviour of the (γ, I) plot outside the spikes as seen in Fig. 5(i).

3 Stochastic acceleration

In the model proposed by Benz (1977), electrons are accelerated stochastically in a slab, surrounding a current sheet, of area A, thickness $2L$, plasma density n, filled by waves of
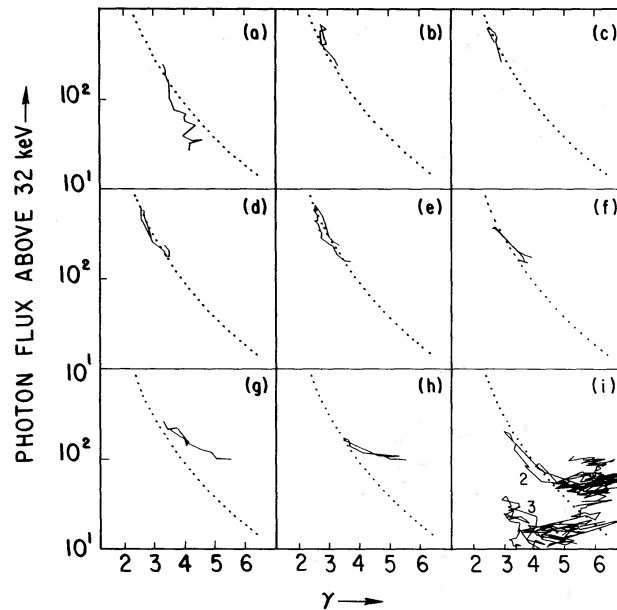

Figure 5. Loci of I_* $(\text{cm}^{-2}\text{s}^{-1})$ (with $\epsilon = E_* = 32\,\text{keV}$) versus γ for the event of 1980 June 7 plotted separately for each of the time intervals (a) rise, (b)–(h) seven main spikes and (i) remainder of event, shown in Fig. 4. Superposed (dashed curve) is the best stochastic wave model fit to the first five spikes. Note the deviation in spikes (g) and (h) to larger γ (or larger I_*). The anticorrelation trends labelled 2 and 3 in (i) correspond to the second and third sets of impulsive spikes discussed by Kiplinger *et al.*

total energy density W (*cf.* Hoyng 1975; Hoyng *et al.* 1980). Electrons in this slab lose energy by Coulomb collisions and escape from the edges of the slab to emit thick target hard X-rays in the chromosphere. In Benz's (1977) original model, W comprised Langmuir waves — an option which has since been heavily criticized (e.g. Vlahos & Papadopoulos 1982) but the important features of Benz's (1977) treatment apply equally to stochastic acceleration by any type of wave so we need not be specific here. For any such situation, evolution of the non-relativistic electron distribution function $f(E, t)$ is described, provided it remains isotropic, by the continuity equation (e.g. Benz 1977)

$$\left(\frac{\partial}{\partial t} + \frac{\partial}{\partial x} v\right) f(E) = \frac{\partial}{\partial E}\left(aE \frac{\partial}{\partial E} \frac{f(E)}{E^{1/2}}\right) + \left(\frac{\partial f}{\partial t}\right)_{\text{coll.}} \tag{1}$$

where the (diffusion) coefficient a depends on the wave density W and its distribution over wavenumber k according to (Kaplan, Pikelner & Tsytovich 1974)

$$a = \pi^2 e^2 w_{\text{pe}}^2 \frac{(2m)^{1/2}}{E} \int_{k_0}^{\infty} \frac{W_k dk}{k^3} \tag{2}$$

where $k_0 = w_{\text{pe}}(2m/E)^{1/2}$.

In his analysis, Benz (1977) assumes W_k is a constant W_0 over the range of integration to obtain $a = \pi^2 e^2 W_0/[2(2m_e)^{1/2}]$ though in fact no essential change in results occurs for the more general assumption (*cf.* Kaplan *et al.* 1974) $W_k = W_0(k/k_0)^{-\beta}$ which yields

$$a = \frac{\pi^2 e^2 W_0}{(\beta + 2)(2m_e)^{1/2}} \tag{3}$$

which is just a rescaling of W_0 compared to Benz's case of $\beta = 0$. The collision term in (1) can be written (Benz 1977)

$$\left(\frac{\partial f}{\partial t}\right)_{\text{coll}} = b \frac{\partial}{\partial E} \frac{f(E)}{E^{1/2}} \tag{4}$$

where

$$b = \frac{8\pi e^4 \Lambda n}{(2m_e)^{1/2}}. \tag{5}$$

To solve (1), Benz assumes that the region is in a steady state ($\partial/\partial t = 0$) and replaces $\partial/\partial x$ by $1/2L$ to obtain a differential (Bessel) equation for $f(E)$. Retention of exact $\partial/\partial E$ terms, however, seems unjustified and unnecessary when $\partial/\partial x$ terms are so approximated and here we reach the same results as Benz (1977) by adoption of characteristic gradient scales in both x and E. That is, spatial variations are characterized by a scale (escape) length L such that

$$\frac{\partial}{\partial x} \simeq \frac{1}{2L} \qquad \text{with } 2L \simeq \frac{f}{\partial f/\partial x} \tag{6}$$

and the spectral distribution is characterized by a scale energy ΔE such that

$$\frac{\partial}{\partial E} = \frac{1}{\Delta E} \qquad \text{with } \Delta E \simeq \frac{f}{\partial f/\partial E}. \tag{7}$$

Substitution of (3)–(7) in (1) leads to an *algebraic* equation for ΔE (as a function of E) namely

$$a \left(\frac{E}{\Delta E} \right)^2 + b \left(\frac{E}{\Delta E} \right) - cE^2 = 0 \tag{8}$$

where

$$c = \frac{1}{(2m)^{1/2}L}. \tag{9}$$

In (8) we recognize $E/\Delta E$ as a measure of the logarithmic slope of the electron number spectrum, namely, for the case of a power-law model $f(E) \propto E^{-\Delta}$, by (7)

$$\frac{E}{\Delta E} = \frac{E}{f} \frac{\partial f}{\partial E} = \frac{\partial \ln f}{\partial \ln E} = -\Delta \tag{10}$$

or in terms of the more usual spectral index $\delta = \Delta - 1/2$ for the electron *flux* spectrum, $E/\Delta E = -(\delta + 1/2)$, related to the thick target *photon* flux spectral index γ by $\delta = \gamma + 1$ (Brown 1971). (Benz does not treat these relationships between Δ, δ and γ correctly, essentially assuming $\Delta \sim \delta \sim \gamma$, and so obtains results which are quantitatively incorrect – unless $\gamma \gg 1$ – though qualitatively equivalent to ours.) Substitution of these relationships together with (10) in (8) yields a quadratic in γ with solution

$$\gamma = -{}^3\!/_2 + d + (d^2 + e^2)^{1/2} \tag{11}$$

$$d = \frac{b}{2a} = \frac{4\Lambda}{\pi}(\beta + 2)e^2 \frac{n}{W_0} \tag{12}$$

and

$$e = \left(\frac{c}{a} \right)^{1/2} E = \frac{(\beta + 2)^{1/2}}{\pi e} \frac{E}{(W_0 L)^{1/2}}. \tag{13}$$

For the acceleration process to be effective, it is necessary for the Coulomb collisional depth of the turbulent slab to be small compared to its effective (wave) collisional depth. This requires (*cf.* Benz 1977) $e \gg d$ so that (11) approximates to

$$\gamma \simeq -\frac{3}{2} + e + d = -\frac{3}{2} + \frac{2^{1/2}E_*}{\pi e(W_0 L)^{1/2}} + \alpha \left(\frac{2^{1/2}E_*}{\pi e(W_0 L)^{1/2}} \right)^2 \tag{14}$$

where

$$\alpha = 4\pi e^4 \Lambda nL/E_*^2 \tag{15}$$

measures the Coulomb collisional depth of the turbulent slab for electrons of energy E_*. For a prescribed α, equation (14) implies that as the turbulent slab parameters (W_0 and L) vary (due presumably to global MHD processes governing the current layer or layers), the hard X-ray spectral slope $\gamma = \delta - 1$ due to escaping electrons should be uniquely determined by the instantaneous value of $W_0 L$. Benz then further argues, on the basis of Tsytovich (1972), that the *rate* of acceleration of electrons above E_* should be proportional to $W_0 L$ provided the sheet area A remains constant. That is, the thick target injection rate $\mathscr{F}_* \, (\text{s}^{-1})$ above

energy E_* is taken to be

$$\mathscr{F}_* = K_1(W_0L) \tag{16}$$

with K_1 proportional to A.

To relate this to the resulting thick target X-ray flux, we will use the simplest (Kramer's) bremsstrahlung cross-section $Q_0/\epsilon E$ per unit photon energy ϵ, which will be quite adequate for estimating variations in spectral hardness (in terms of γ) for the order of theoretical description used here. The relevant relationship is easily found to be

$$I_* = I(\epsilon = E_*) = \frac{Q_0}{8\pi^2 e^4 R^2 \Lambda} \frac{\mathscr{F}_* E_*}{(\gamma - 1)^2} \tag{17}$$

where $R = 1\,\text{AU}$ and I_* is the total X-ray flux at the Earth above photon energy $\epsilon = E_*$ so that with $K = K_1 Q_0 E_*/(8\pi^2 e^4 R^2 \Lambda)$, (16) and (17) imply

$$I_* = K(W_0L)/(\gamma - 1)^2 \tag{18}$$

which is again a function only of W_0L and of $\gamma(W_0L)$ in the Benz interpretation. It follows from (14) and (18) that the stochastic wave acceleration model predicts a unique relationship (for prescribed α) between variations in X-ray flux and spectral index viz., by elimination of W_0L,

$$\log_{10}I_* = \log_{10}C - 2\log_{10}[(\gamma - 1)(\gamma + 3/2)] + 2\log_{10}\{\tfrac{1}{2} + \tfrac{1}{2}[1 + 4\alpha(\gamma + \tfrac{3}{2})]^{1/2}\} \tag{19}$$

with $C = (\beta + 2)E_*^2 K/\pi^2 e^2$.

In Fig. 6 we show the predicted form of $\log_{10}I_*/C$ versus γ for various α. It should be noted that though increasing α raises $\log_{10}I_*$ it has comparatively little effect on the *slope* of the curve — specifically the change in $\log_{10}I_*$ (i.e. the mean slope) between prescribed abscissae γ_1 and γ_2 due to the term in (19) containing α tends to the finite limit $\log_{10}$ $[(\gamma_1 + 3/2)/(\gamma_2 + 3/2)]$ even as $\alpha \to \infty$, which is small compared to the effect of the second term in (19). Clearly (19) predicts that I_* and γ should anticorrelate through the event as W_0L varies, in qualitative agreement with the observed trend. We now consider the extent of agreement between the model and the data (purely for purposes of comparison with Benz
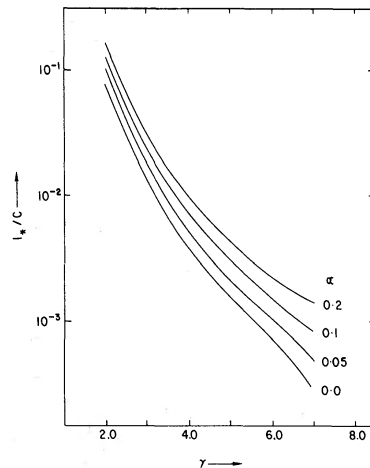

Figure 6. Behaviour of the γ, I_* locus predicted by the stochastic acceleration/thick target injection model described in Section 3 (after Benz 1977) for various values of the slab collisional thickness α. The intensity axis is scaled relative to the constant C which depends mainly on the area of the acceleration slab.

results we will henceforth take $\beta = 0$ noting that other values simply rescale the interpretation of C).

4 Comparison of model and data

4.1 EVENT OF 1980 MARCH 29

Relationship (19) and Fig. 6 shows that the *slope* of $\log_{10} I_*$ versus γ is independent of C and only very weakly dependent on α. We have therefore performed an adjustment of C until we obtain the best eyeball match of Fig. 6 with the data on the March 29 event shown in Fig. 2. A surprisingly good model fit to the data is seen to be obtained for any of the α values shown in Fig. 6, with suitably adjusted C, though $\alpha \simeq 0.1$ seems marginally better than the others, with a corresponding $C = 1.4 \times 10^4 \, \text{cm}^{-2} \, \text{s}^{-1}$. While recognizing that the value of α is poorly determined by the data, if we take this best fit as a reasonable estimate of the actual value then (15) with $E_* = 32 \, \text{keV}$ implies

$$n_{12} L_7 \simeq 2 \tag{20}$$

where $n = 10^{12} n_{12} \, \text{cm}^{-3}$, $L = 10^7 L_7 \, \text{cm}$. The (well-determined) value of γ at each instant then implies the value of $W_0 L$ by (14) — in particular, at burst peak, $\gamma = 3.1$ implies (*cf.* Benz)

$$W_0 L_7 \simeq 2 \times 10^{-5} \, \text{erg} \, \text{cm}^{-2}. \tag{21}$$

Further information is contained in the value of I_* at peak which by (17) implies a peak electron acceleration rate above 32 keV of

$$\mathcal{F}_* \simeq 2 \times 10^{35} \, \text{s}^{-1} \tag{22}$$

which is in turn related to the time t_a taken to accelerate an average electron in the turbulent slab, equal to the total number instantaneously in the slab divided by the total rate of electron acceleration, viz.

$$t_a = nAL/\mathcal{F}_* \simeq 10 A_{17} \, \text{s} \tag{23}$$

where we have used results (20) and (22) and set the slab area $A = 10^{17} A_{17} \, \text{cm}^2$.

For stability of the neutralizing return current driven by the electrons escaping to the thick target region, we further typically require (e.g. Brown & Hayward 1982)

$$n_{12} A_{17} T_7^{1/2} \gtrsim 10^{-2} \mathcal{F}_{35} \simeq 2 \times 10^{-2} \tag{24}$$

where we have again used (22) and set $\mathcal{F}_* = 10^{35} \mathcal{F}_{35} \, \text{s}^{-1}$. Plausible values $A_{17} \simeq 1$ and $T_7 \simeq 1$ satisfy (24) for $n \gg 10^{10} \, \text{cm}^{-3}$ which is also required for the slab thickness to be reasonably small (20).

Thus the dynamic spectral behaviour of the March 29 event seems to be well explained along similar lines to those proposed by Benz but for a generalized stochastic wave process. There remains of course the fundamental problem of efficiency (*cf.* Hoyng *et al.* 1980) in accelerating the large flux (22) (i.e. in the large value of C), though the acceleration time (23) per electron does not seem too demanding. In addition there are small but significant variations in the (γ, I_*) locus of this event from a unique track (Fig. 2). These may be explained by some of the factors discussed below.

4.2 EVENT OF 1980 JUNE 7

We have followed a similar procedure to that in 4.1 for the June 7 event. We find that the (γ, I_*) loci for the first five [Fig. 5(b)–(f)] of the seven spikes can be well described by a model locus of type (19) with single values of $C \simeq 1.6 \times 10^4 \, \text{cm}^{-2} \, \text{s}^{-1}$ and of $\alpha \simeq 0.05$, as shown by the dotted line on Fig. 5(a)–(g). The sixth and seventh spikes of the first set do fall along a common (γ, I_*) locus with these five spikes, but one which has higher γ at decreasing I_* than is compatible with any model locus of the type considered here. For the moment we consider (in the same way as 4.1) only the five spikes which dominate the others in intensity and later discuss possible factors affecting the later behaviour. We also note that the rising phase of the event [Fig. 5(a)] shows a distinct (γ, I) behaviour, presumably characteristic of the onset of acceleration as discussed later also.

Firstly, we have for this event by (15), with $\alpha \simeq 0.05$

$$n_{12} L_7 \simeq 1 \tag{25}$$

while by (14) from the value of $\gamma \simeq 2.6$ at event peak we obtain at that time

$$W_0 L_7 \simeq 2 \times 10^{-5} \, \text{erg} \, \text{cm}^{-2} \tag{26}$$

again comparable to Benz's results. The thick target flux at the peak of this event above 32 keV is

$$\mathscr{F}_* \simeq 7 \times 10^{35} \, \text{s}^{-1} \tag{27}$$

and corresponding acceleration time [using (25) and (23)]

$$t_a = 1.5 \, A_{17} \, \text{s.} \tag{28}$$

The return current stability condition in this case is

$$n_{12} A_{17} T_7^{1/2} \gtrsim 7 \times 10^{-2} \tag{29}$$

implying densities $n \gtrsim 10^{11} \, \text{cm}^{-3}$ for plausible A, T.

The June 7 data in fact deviate from the model prediction in two significant ways. Firstly there is the flattening of the (γ, I_*) locus during the sixth and seventh spikes of the first set and in the subsequent evolution. Secondly the (γ, I_*) evolution, even during the first five spikes, does not strictly follow a unique path – in particular there is a 'hysteresis' effect (*cf.* Kiplinger *et al.* 1983) between rise and fall of each spike such that lower values of γ occur during the fall than on the rise, at the same value of I_*. Considering first the flattening of the locus in the decay phase, several possible interpretations suggest themselves. In terms of the model itself, it is clear from Figs 5 and 6 that, no matter how high α is, steady-state collisional effects cannot flatten the locus as much as is observed. On the other hand, if α were to increase in time through the event (due to increasing density n or thickness L of the turbulent slab), then the locus could flatten as observed. Fig. 5 indicates that α would have to increase from about 0.05 to about 0.2 during event decay for this explanation to work – i.e. a fourfold density increase which seems physically implausible. An alternative and more likely explanation is an increase in slab area in the decay phase (i.e. while $W_0 L$ is declining) which increases I_* without change in γ, for a given $W_0 L$ (*cf.* equation 16). Comparison of Figs 5 and 6 here shows that a 50 per cent increase in slab area would suffice to explain the observed flattening. A less interesting interpretation, but one which requires further investigation, is that the flattening is not due to an increase of I_* for a given γ in terms of the model, but rather due to an increase in γ above the model value by addition of softer

emission to the thick target component. In particular, the HXRBS spectrum contribution from a hot thermal plasma at a few times $10^7 K$ has been shown by Gabriel *et al.* (1984) to be substantial in some flares to above 50 keV energies. A thermal contribution of this sort, rising during the decline in the impulsive spikes could modify the model June 7 (γ, I_*) locus as discussed above.

Considering 'hysteresis' effects, these must involve some time-dependent parameter (without which the locus would just be reversible). Collisional effects can be time-dependent in two ways. First, the density n (hence α) may differ between rising and falling phases of $W_0 L$. For this interpretation the observed sense of hysteresis would require that the density (i.e. α) should rise with rising $W_0 L$ (*cf.* Figs 5 and 6) which is the plausible sense — i.e. compression of the slab region by MHD variations would be expected to enhance the total wave energy ($\sim W_0 L$) as well as the density. Secondly, if the changes in $W_0 L$ occur on a time-scale shorter than relevant collisional relaxation times in the slab, our steady-state description becomes invalid. These times include the time-scale $t_1 \simeq E_*^{3/2}/b \simeq 2 \times 10^{-2} (E_*/32 \, keV)^{3/2} n_{12} s$ for the fast electron spectrum to be modified by collisions and the time-scale (*cf.* Benz 1977) $t_2 \simeq 2 (E_*/32 \, keV)^{5/2}/n_{12} T_7 s$ for collisional replenishment of the Maxwellian tail required to supply the electrons needed for turbulent acceleration (Benz — personal communication). The longer time-scale t_2 is the only one relevant, for the high densities considered here, on the time-scale of spike durations. The time delay in filling the Maxwellian tail will tend to make the spike spectrum softer during rise than decay, as observed, if $t_2 \gtrsim$ the spike duration which is of order 8 s, implying $n_{12} T_7 \lesssim 0.25$. Another factor is the rising thermal contribution to the spectrum already discussed. This would tend to make the spectrum softer on the decay than on the rise of each spike and so act in the opposite direction to the other effects above. Similar comments apply to the small 'hysteresis' effects in the March 29 data.

Lastly, we note that although the data are considerably noisier, the second and third sets of spikes reported by Kiplinger *et al.* (1983) show evidence of a similar underlying behaviour [just visible in Fig. 5(i)] in the (γ, I_*) locus to the first set but with values of C reduced by about a factor of 3 for the second set and a factor of 10 for the third set. Since C depends essentially only on the slab area (*cf.* equation 19), these observations suggest the recurrence of the phenomena producing the seven main spikes but in a more limited region of magnetic reconnection.

5 Discussion and conclusions

We have shown that stochastic acceleration of thick target electron beams in a dense plasma slab, containing a turbulent wave spectrum of variable wave level and/or thickness, as proposed by Benz (1977), provides a reasonable description of the dynamic hard X-ray spectral evolution of the events of 1980 March 29 and June 7. In addition we have shown how this interpretation provides constraints on plasma parameters in the slab, and discussed possible factors contributing to deviations between the data and the theory in its simplest form. We do not claim that this interpretation is either complete or unique — alternative explanations may well be feasible. In particular the thermal model (Mätzler *et al.* 1978) involving adiabatic density and temperature variations also reproduces the (γ, I_*) data trend at least in a gross sense (*cf.* Kiplinger *et al.* 1983). Comparison of the acceptability of these two and any other interpretations [such as electron precipitation by decimetric maser action in a trap (Melrose & Dulk 1982)] should be the subject of a more comprehensive study incorporating microwave and soft X-ray data as well as the hard X-ray dynamic spectrum.

In terms of non-thermal models, however, stochastic acceleration is of particular theo-

retical interest at present. It has been shown recently (Holman 1983; Spicer 1983), on electrodynamic grounds, that acceleration of beams with the fluxes typical of thick target data interpretations is very difficult to achieve by direct acceleration in an electric field induced by magnetic field changes. Models in which the 'beam' is formed by escape of electrons from a region with an almost isotropic electron distribution, such as in stochastic turbulent acceleration, do not present this problem since there is no strong beam current in the acceleration region.

Acknowledgments

References

Benz, A. O., 1977. *Astrophys. J.*, **211**, 270.
Brown, J. C., 1971. *Solar Phys.*, **18**, 689.
Brown, J. C. & Hoyng, P., 1975. *Astrophys. J.*, **200**, 734.
Brown, J. C. & Hayward, J., 1982. *Solar Phys.*, **80**, 129.
Crannell, C. J., Frost, K. J., Mätzler, C., Ohki, K. & Saba, J. L., 1978. *Astrophys. J.*, **223**, 620.
Dennis, B. R., Frost, K. J. & Orwig, L. E., 1981. *Astrophys. J.*, **244**, L153.
Gabriel, A. H., Bely-Dubau, F., Sherman, J., Orwig, L., Schrijver, J., 1984. *Adv. Space Res.*, in press.
Holman, G. E., 1983. *Plasma Instabilities and Unstable Current Systems in Astrophysics, IAU Symp. No. 102*, Reidel, Dordrecht, Holland.
Hoyng, P., 1975. *Ph.D. thesis*, Utrecht.
Hoyng, P., Brown, J. C. & van Beek, H. F., 1976. *Solar Phys.*, **48**, 197.
Hoyng, P., Duijveman, A., van Grunsven, T. F. J. & Nicolson, D. R., 1980. *Astr. Astrophys.*, **91**, 17.
Hudson, H. S., Canfield, R. C. & Kane, S. R., 1978. *Solar Phys.*, **60**, 137.
Kane, S. R. & Anderson, K., 1970. *Astrophys. J.*, **162**, 1003.
Kane, S. R., 1974. *Coronal Disturbances, IAU Symp. No. 57*, p. 105, ed. Newkirk Jr., G., Reidel, Dordrecht, Holland.
Kane, S. R., Kai, K., Kosugi, T., Enome, S., Landecker, P. B. & McKenzie, D. L., 1983. *Astrophys. J.*, **271**, 376.
Kaplan, S. A., Pikelner, S. B. & Tsytovich, V. N., 1974. *Phys. Repts.*, **15**, 1.
Kiplinger, A. L., Dennis, B. R., Frost, K. J. & Orwig, L. E., 1983. *Astrophys. J.*, **273**, 783.
Mätzler, C., Bai, T., Crannell, C. J. & Frost, K. J., 1978. *Astrophys. J.*, **223**, 1058.
Melrose, D. B. & Brown, J. C., 1976. *Mon. Not. R. astr. Soc.*. **176**, 15.
Melrose, D. B. & Dulk, G. A., 1982. *Astrophys. J.*, **259**, 844.
Spicer, D. S., 1983. Preprint.
Tsytovich, V. N., 1972. *An Introduction to the Theory of Plasma Turbulence*, Pergamon Press, Oxford.
Vlahos, L. & Papadopoulos, 1982. *Astrophys. J.*, **252**, L75.